Preparation of a stable CCL5·CCR5·G_i signaling complex for Cryo-EM analysis

Polina Isaikina[1*], Ching-Ju Tsai[2], Ivana Petrovic[1], Marco Rogowski[1], Alexandra Meng Dürr[1] and Stephan Grzesiek[1,*]

Affiliations:
[1] Focal Area Structural Biology and Biophysics, Biozentrum, University of Basel, CH-4056 Basel, Switzerland
[2] Paul Scherrer Institute, CH-5232 Villigen PSI, Switzerland

Keywords:
G protein coupled receptor (GPCR), HIV, membrane protein structure, insect cell expression, chemokine purification, chemokine receptor purification, GPCR•G protein complex assembly

*Address correspondence to:
Polina Isaikina
Focal Area Structural Biology and Biophysics, Biozentrum
University of Basel, CH-4056 Basel, Switzerland
Phone: +41 61 207 20 80
Email: Polina.Isaikina@unibas.ch

Stephan Grzesiek
Focal Area Structural Biology and Biophysics, Biozentrum
University of Basel, CH-4056 Basel, Switzerland
Phone: ++41 61 267 2100
FAX: ++41 61 267 2109
Email: Stephan.Grzesiek@unibas.ch

1 ABSTRACT **3**
2 INTRODUCTION **4**
3 METHODS **7**
3.1 OVERVIEW 7
3.2 CHEMOKINE PRODUCTION 7
3.2.1 Equipment and materials *8*
3.2.2 Reagents *8*
3.2.3 Buffers *9*
3.2.4 DNA construct *9*
3.2.5 Expression *10*
3.2.6 Purification and cyclization of chemokine N-terminus *10*
3.2.7 Quality control *13*
3.3 CHEMOKINE RECEPTOR EXPRESSION AND MEMBRANE PREPARATION 14
3.3.1 Equipment and materials *14*
3.3.2 Reagents *14*
3.3.3 Buffers *15*
3.3.4 DNA construct *15*
3.3.5 Expression and membrane preparation *15*
3.4 CHEMOKINE RECEPTOR PURIFICATION AND COMPLEX FORMATION 18
3.4.1 Equipment and materials *18*
3.4.2 Reagents *18*
3.4.3 Buffers *19*
3.4.4 Receptor purification *19*
3.4.5 Receptor complex formation *20*
3.4.6 Receptor complex purification *21*
3.5 QUALITY CONTROL OF RECEPTOR COMPLEX STABILITY BY GTPγS BINDING ASSAY 22
3.6 PREPARATION OF CRYO-EM GRIDS 23
3.6.1 Equipment and materials *23*
3.6.2 Cryo-EM grid preparation *23*
4 DISCUSSION AND CONCLUSION **24**
5 TABLES **27**
6 FIGURE LEGENDS **28**
7 ACKNOWLEDGMENTS **29**
8 CONFLICT OF INTEREST **29**
9 REFERENCES **30**

1 Abstract

The numerous chemokines and their cognate G protein-coupled chemokine receptors on the surface of leukocytes form a complex signaling network, which regulates the immune response and also other key physiological processes. Currently only a very limited number of structures of chemokine•chemokine receptor complexes have been solved. More structures are needed for the understanding of their mechanism of action and the rational design of drugs against these highly relevant therapeutic targets. Recently, we have determined the cryo-EM structure of the human wild-type CCR5 chemokine receptor, which is also the HIV-1 coreceptor, in its active conformation bound to the chemokine super-agonist [6P4]CCL5 and the heterotrimeric G_i protein. The structure provides the rationale for the sequence-activity relation of agonist and antagonist CCR5 chemokine ligands.

In this chapter, we present a detailed protocol for the preparation of the active agonist chemokine•CCR5•G_i complex for cryo-EM studies including quality controls and caveats. As such the protocol may serve as starting point for structural and biophysical studies of other chemokine•receptor receptor complexes.

2 Introduction

Chemokines and their cognate receptors form a complex signaling system comprising more than 50 chemokines and 24 receptors in humans (Bachelerie et al., 2014). They play a crucial role in a wide range of physiological processes mainly related to chemotactic trafficking of leukocytes from the blood to the tissues and around the lymphatic system (Scurci et al., 2018). As such, the chemokine system is strongly implicated in many pathologies including AIDS (Brelot and Chakrabarti, 2018), COVID-19 (Chua et al., 2020) and cancer (Aldinucci and Casagrande, 2018; Kraus et al., 2021; Ortiz Zacarías et al., 2021). The chemokine/chemokine receptor pairs involved in specific pathologies constitute highly relevant therapeutic targets (Lai and Mueller, 2021; Ortiz Zacarías et al., 2021). Despite extensive efforts, to date only three drugs targeting chemokine receptors have been approved for clinical use (Lai and Mueller, 2021; Zhao et al., 2019). The primary reason is apparently a still limited understanding of the underlying interactions within the chemokine system.

Chemokines are a subgroup of soluble signaling proteins of 8–12 kDa size within the large cytokine family. They are divided into 4 subfamilies (CC, CXC, CX3C, and XC) according to the spacing and presence of structurally important N-terminal cysteine residues, which form disulfide bonds to other conserved cysteines in the protein core (Stone et al., 2017). Despite their functional diversity and relatively low sequence homology, the three-dimensional structures of chemokines are highly similar (Miller and Mayo, 2017). While many chemokines form dimers and often higher oligomers, they bind to their membrane receptors as monomers. In contrast, chemokines interact strongly in oligomeric form with a ‘second type of receptor’ on the cell surface (Handel and Dyer, 2021; Stone et al., 2017), the glycosaminoglycans (GAGs). This interaction is critical for leukocyte recruitment and is thought to create localized pools of chemokines that can then bind to their cognate membrane receptors (Handel and Dyer, 2021).

Dimerization of CC chemokines (CCLs) occurs via intermolecular β-sheet formation of their unstructured N-termini, which precludes receptor binding for steric reasons (Duma et al., 2007; Handel and Dyer, 2021). Higher

oligomerization of CC chemokines occurs via additional interactions involving their C-terminal helix and second β-strand (Wang et al., 2011). In contrast, CXC chemokines (CXCLs) dimerize via an intermolecular extension of their antiparallel β-sheet (Miller and Mayo, 2017), which appears compatible with receptor binding (Handel and Dyer, 2021; Liu et al., 2020).

The dissociation constant of chemokine dimers is typically in the low micromolar range and pH- as well as temperature-dependent (Chen et al., 2020; Duma et al., 2007; Fernando et al., 2004; Ravindran et al., 2013). To achieve high homogeneity of chemokine-chemokine receptor complex preparations for structural studies, it is essential that chemokines bind predominantly as monomers to their receptors. This is best achieved under conditions of low concentrations, suitable pH and by a high affinity (nanomolar) of the chemokine to the receptor.

Chemokine receptors are integral membrane proteins belonging to the class A of G protein-coupled receptors. Most receptors bind chemokines exclusively from one family (CC, CXC, CX3C, XC) and are classified accordingly (CCR, CXCR, CX3CR, XCR). This selectivity apparently results from distinct orientations of the chemokine N-terminus induced by the N-terminal cysteine motif (Wedemeyer et al., 2020). Within one family, the receptor-chemokine specificity is often not very strong, as many chemokines bind multiple chemokine receptors and many receptors bind multiple chemokines (Bachelerie et al., 2014). An additional degree of complexity stems from post-translational modifications of the receptor such as sulfation and O-glycosylation, which contribute to chemokine affinity (Duma et al., 2007; Kessler et al., 2020; Szpakowska et al., 2012). Moreover, chemokine receptors can form homo- and heterodimers, as well as higher-order oligomers (D'Agostino et al., 2020). The functional implications of receptor and chemokine oligomer formation are currently not well understood. It is clear, however, that both post-translational modifications and oligomerization vastly expand the arsenal of possible chemokine-receptor interactions. This makes the chemokine system a challenging target for structural biology and drug development.

A number of structures of chemokine receptors in their inactive conformation in complexes with small-molecule ligands have been solved by X-ray crystallography (Apel et al., 2019; Jaeger et al., 2019; Oswald et al., 2016; Peng et al., 2018; Tan et al., 2013; Wu et al., 2010; Zheng et al., 2016). In contrast, due to the larger size and increased dynamics of receptor complexes with intact chemokines, until recently only five full chemokine•chemokine receptor complex structures have been available (Figure 1). Two of these complexes, vMIP-II•CXCR4 (Qin et al., 2015) and [5P7]CCL5•CCR5 (Zheng et al., 2017), are in the inactive receptor conformation. The remaining three are all complexes of the viral chemokine receptor US28. US28 is a special case, since it is constitutively active, and its inverse-agonist-bound as well as its apo structures (Burg et al., 2015; Miles et al., 2018) are all in active conformations. The situation has changed in the last two years due to the advances in cryo-EM technology, which enabled the structure determination of five further human chemokine•receptor complexes in their active conformation bound to G proteins (Isaikina et al., 2021; Liu et al., 2020; Wasilko et al., 2020; Zhang et al., 2021).

One of these is the complex of the wild-type human CC chemokine receptor 5 (CCR5) with the chemokine super-agonist [6P4]CCL5, the heterotrimeric G_i protein and the stabilizing antibody fragment Fab16 (Isaikina et al., 2021). Since its discovery in 1996 (Combadiere et al., 1996; Raport et al., 1996; Samson et al., 1996), CCR5 has been under extensive investigation due to its major role in HIV (Alkhatib, 2009), inflammation (Martin-Blondel et al., 2016), the pathology of cancer (Aldinucci et al., 2020), and COVID-19 (Chua et al., 2020). The sequence of [6P4]CCL5 differs from wild-type CCR5 by several amino acid substitutions in its flexible N-terminus that increase its agonistic efficacy and the affinity to CCR5. The comparison of the active [6P4]CCL5•CCR5•G_i complex to the inactive, antagonist chemokine [5P7]CCL5•CCR5 complex revealed the rationale for the sequence-activity relation of agonist and antagonist chemokines (Isaikina et al., 2021). Two additional structures of CCR5•G_i bound to CCL3 and CCL5 have now been published (Zhang et al., 2021). The latter complexes were stabilized by fusing the chemokine C-terminus to the N-term inus of CCR5 and further mutations.

We present here a step-by-step protocol for the preparation of the complex between [6P4]CCL5, wild-type CCR5, G_i, and the stabilizing Fab16, which led to its successful structure determination (Isaikina et al., 2021). We include pertinent quality control steps and point out difficulties in the hope that the protocol may serve as a model for the preparation of other active chemokine•chemokine receptor•G protein complexes for cryo-EM structure determination and other biophysical studies.

3 Methods

3.1 Overview

A schematic diagram of the [6P4]CCL5•CCR5•Gi•Fab16 complex preparation for cryo-EM analysis including quality control steps is shown in Figure 2. The individual components [6P4]CCL5, CCR5, $G\alpha_i$, Gβγ, and Fab16 are produced separately and then allowed to form the complex. Details of the production of the engineered chemokine CCL5 super-agonist analog [6P4]CCL5 (Gaertner et al., 2008) and the wild-type receptor CCR5 are given below, whereas detailed protocols for the production of $G\alpha_i$ (Sun et al., 2015), Gβγ (Maeda et al., 2014), and Fab16 (Tsai et al., 2019) have been presented in the indicated references.

3.2 Chemokine production

This section describes the expression and purification of the engineered super-agonist chemokine [6P4]CCL5. Other chemokines may be obtained in an analogous manner. [6P4]CCL5 is expressed in *Escherichia coli (E. coli)* as an N-terminal thioredoxin/His tag fusion protein (Figure 3A). A summary of the main production steps is shown in Figure 3B.

In brief, the expressed fusion protein is unfolded by 6 M guanidine hydrochloride and then purified by nickel-affinity chromatography, followed by reduction of its two disulfide bonds by 2-mercaptoethanol. Refolding and simultaneous formation of disulfide bonds is induced by adding the protein to a refolding redox buffer containing a mixture of reduced and oxidized glutathione. After refolding, the fusion protein is cleaved by enterokinase, resulting in

[6P4]CCL5 with a blunt N-terminus starting at residue glutamine-0 (Q0). The fusion partner is then separated by reversed-phase chromatography. The N-terminal glutamine spontaneously cyclizes to pyroglutamate to form the mature [6P4]CCL5 (Gaertner et al., 2008). Full cyclization of the N-terminus and overall quality of the protein is assayed by either mass spectrometry (MS; Figure 3C) or NMR spectroscopy (Figure 3D).

3.2.1 Equipment and materials

- Temperature-controlled incubator shaker (Infors HT, Multitron)
- 1-L Erlenmeyer flask
- 5-L Erlenmeyer flask
- French pressure cell and press (Spectronic Instruments, FA-031)
- Ultracentrifuge (Beckman Coulter, Optima XE)
- Membrane filter (Merck, MF-Millipore, 0.45-µm pore size)
- Tabletop centrifuge (Eppendorf, 5430 R)
- Centrifugal filter units (Merck, Amicon Ultra-4 and -15)
- Pressure-based stirred concentrator cell (Merck, Amicon)
- Ultrafiltration polyether sulfone-based membrane discs [Merck, Biomax, 10-kDa molecular weight cut-off (MWCO)]
- Dialysis tubes (Spectrum Chemical, Spectra/Por, 12–14 kDa MWCO)
- Sodium dodecyl sulphate-polyacrylamide gel electrophoresis (SDS-PAGE) system (Bio-Rad)
- Precast 4–20% gradient SDS-PAGE gels (Bio-Rad)
- Fast protein liquid chromatography (FPLC) system (Cytiva, ÄKTA pure)
- Nickel affinity column (Cytiva, HisTrap HP)
- Preparative HPLC system (Beckman Coulter, System Gold)
- C4 reversed-phase HPLC column 250 x 21.20 mm, 10 micron, 300 Å (Phenomenex)
- Freeze dryer (Thermo Fisher Scientific, Savant)
- Microvolume spectrophotometer (Thermo Fisher Scientific, NanoDrop)
- C4 micro spin column for MS analysis (The Nest Group, MicroSpin)
- Electrospray ionization time-of-flight (ESI-TOF) mass spectrometer (Bruker, microTOF$_{LC}$)
- High-field (≥500 MHz) NMR spectrometer (Bruker, AVANCE)

3.2.2 Reagents

- *E. coli* strain BL21 (DE3)
- Lysogeny broth (LB) medium (Miller)
- *E. coli* minimal medium (Cai et al., 1998) and ^{15}N-labeled ammonium chloride for production of ^{15}N-labeled chemokine and NMR quality control
- Isopropyl β-D-thiogalactopyranoside (IPTG)
- Guanidine hydrochloride (GuHCl)

- Sodium chloride
- Sodium acetate (NaOAc)
- Tris-(hydroxymethyl)-aminomethane (Tris) hydrochloride
- L-arginine hydrochloride
- Glutathione, reduced (GSH) and oxidized (GSSG)
- Enterokinase [either commercial (New England biolabs) or produced in-house - an optimized protocol is available upon request]
- Trifluoroacetic acid (TFA)
- Acetonitrile (ACN)
- 2-mercaptoethanol
- Ethylenediaminetetraacetic acid (EDTA)

3.2.3 Buffers

Note: all solutions are prepared using ultrapure water (Milli-Q, resistivity ≥18.2 MΩ/cm). Buffer pH values are indicated for the temperature at which they are used.

- Resuspension buffer: 6 M GuHCl, 200 mM NaCl, 50 mM Tris, pH 8.0
- HisTrap elution buffer: 6 M GuHCl, 200 mM NaCl, 60 mM NaOAc, pH 4.0
- Refolding buffer: 550 mM L-arginine hydrochloride, 200 mM NaCl, 1 mM EDTA, 1 mM GSH, 0.1 mM GSSG, 50 mM Tris, pH 8.0
- Cleavage buffer: 200 mM NaCl, 2 mM $CaCl_2$, 20 mM Tris, pH 8.0
- Reversed-phase buffer A: 0.1% TFA
- Reversed-phase buffer B: 0.085% TFA in 90% ACN
- MS buffer A: 10% ACN, 0.1% formic acid
- MS buffer B: 90% ACN, 0.1% formic acid

3.2.4 DNA construct

A DNA construct of [5P14]CCL5 harboring an N-terminal thioredoxin fusion partner and an enterokinase cleavage site cloned into a pET32a vector (Figure 3A) was a gift from Prof. P. LiWang (UC Merced).

The DNA sequence of the [5P14]CCL5 construct was mutated by Quik-Change™ (Stratagene) polymerase chain reaction to obtain the [6P4]CCL5 construct. Its final amino acid sequence including fusion partners (chemokine sequence in bold) is:

MSDKIIHLTDDSFDTDVLKADGAILVDFWAEWCGPCKMIAPILDEIADEYQGKLTVAKLNIDQ
NPGTAPKYGIRGIPTLLLFKNGEVAATKVGALSKGQLKEFLDANLAGSGSGHMHHHHHHSSGL
VPRGSGMKETAAAKFERQHMDSPDLGTDDDDK**QGPPGDIVLACCFAYIARPLPRAHIKEYFYT**
SGKCSNPAVVFVTRKNRQVCANPEKKWVREYINSLEMS

In our hands, this construct worked best for the production of various chemokine analogs. An alternative construct containing an N-terminal protein G followed by an enterokinase cleavage site worked well for the production of CCL5-E66S and [5P12]CCL5 (Duma et al., 2007; Wiktor et al., 2013). However, cleavage of the fusion partner from [6P4]CCL5 and [5P14]CCL5 (data not shown) was inefficient in the latter, presumably due to the burial of the cleavage site by the differing N-termini.

3.2.5 Expression

- Transform *E. coli* BL21(DE3) strain with the [6P4]CCL5-encoding plasmid and plate it on an LB agar plate containing 100 µg/mL ampicillin. Incubate the plate overnight at 37 °C.
- Inoculate a single colony from the LB agar plate in 100–120 mL LB broth containing 100 µl/mL ampicillin and grow overnight at 37 °C at a shaking speed of 150 rpm. Note that for producing ^{15}N-labeled protein, bacteria are grown in minimal medium supplemented with ^{15}N-labeled ammonium chloride.
- Use 50–60 mL of primary inoculum to inoculate 1.5 L LB broth containing 100 µL/mL ampicillin in a 5-L Erlenmeyer flask [initial optical density at 600 nm (OD_{600}) ≅ 0.1] at 37 °C and 150 rpm.
- Lower the temperature to 22 °C once OD_{600} reaches 0.5–0.6 (this typically takes ~2–2.5 h).
- When OD_{600} reaches 0.8, induce the protein expression with 1.0 mM IPTG and grow the cells for another 20 hours.
- Harvest the cells by centrifugation at 3,000 *g* for 25 min. Discard the supernatant and store the pellet at -80 °C or proceed directly to purification.

3.2.6 Purification and cyclization of chemokine N-terminus

All purification steps are performed at 4 °C or on ice, unless indicated otherwise.

- Resuspend the cell pellet (~10 g) in 100 mL resuspension buffer and apply the sample to a French press. Repeat this step twice. Note that the 6 M GuHCl of the resuspension buffer denatures the chemokine.

- Centrifuge the resulting lysate at 27,000 *g* for 1 h and collect the supernatant.
- Add another 100 mL of resuspension buffer and filter the suspension through a 0.45-µm filter. Apply the filtrate on the FPLC system to an equilibrated, pre-packed 5-mL Ni affinity column at a flow rate of 0.8 mL/min.
- Wash the column with 10 column volumes (CV) of resuspension buffer at a flow rate of 1 mL/min, then elute the protein with 3–4 CV of HisTrap elution buffer at a flow rate of 0.8 mL/min.
- Add 10 mM of 2-mercaptoethanol to the eluate and mix with end-over-end rotation for 1 hour at room temperature. This step reduces the two disulfide bonds of the chemokine.
- Add the reduced eluate dropwise to a 10–15-fold volume excess of refolding buffer at 4 ˚C and incubate overnight under gentle stirring. During this step, the disulfide bonds are reformed under the control of GSH/GSSG redox system in the buffer and the chemokine is refolded.
- Concentrate the refolded protein to 20–30 mL using a pressure-based concentrator with a polyether sulfone-based ultrafiltration membrane of 10-kDa MWCO.
- Dialyze the concentrated solution against the cleavage buffer in dialysis membrane tubes with a 12–14 kDa MWCO. The volume of the dialysis buffer should be at least 50-fold larger than the sample volume. Change the dialysis buffer twice. Remove any precipitation by centrifugation for 10 min at 25,000 *g*.
- Determine the protein concentration by measuring the absorbance at 280 nm (A_{280}), using the microvolume photometer, then dilute the folded protein to 1.5–2.5 mg/mL.
- Prior to large-scale cleavage of the N-terminal fusion, perform test cleavages with differing amounts of enterokinase:
    - Prepare four 100-µL aliquots of the fusion protein at 2.0 mg/mL.
    - Add enterokinase to the fusion protein aliquots at ratios 1:100, 1:50, 1:25 and 1:10 (w/w) and incubate at room temperature for 16 hours with end-over-end mixing.

    - Analyze the cleavage efficiency by SDS-PAGE to determine the optimal protease:protein ratio, i.e., the minimal amount of enterokinase needed to obtain close to 100% cleavage.
- For large-scale cleavage, add enterokinase to the fusion protein at the determined optimal ratio and incubate at room temperature for 16 hours with end-over-end rotation. Remove trace amounts of precipitate by centrifuging for 10 min at 25,000 *g*. Verify protein cleavage by SDS-PAGE.
- For the final HPLC purification step, adjust the pH of the protein solution to 2.2 using 10% TFA, and then add ACN to a final concentration of 10%.
- Apply the protein to a C4 reversed-phase chromatography column (250 x 21.20 mm, 10 micron, 300 Å, 88 mL, Jupiter) connected to a preparative HPLC system and equilibrated with reversed-phase buffer A. Separate the protein from the fusion tag using the following water/acetonitrile gradient program at a flow rate of 10 mL/min:
    - 0.1 CV: 10% reversed-phase buffer B
    - 0.2 CV: 10% → 20% reversed-phase buffer B
    - 5 CV: 20% → 70% reversed-phase buffer B
    - 0.2 CV: 70% → 100% reversed-phase buffer B
    - 2 CV: 100% reversed-phase buffer B
- Collect the separated protein peaks into different fractions. [6P4]CCL5 elutes at 35–45% of reversed-phase buffer B. Analyze the purity of the eluted fractions by SDS-PAGE.
- Lyophilize the pure chemokine fractions in a freeze dryer. This typically takes approximately 24 hours at a pressure of ~100 µbar.
- Solubilize the lyophilizate in 25 mM phosphate buffer (pH 6) to a concentration of 1.0–1.5 mg/mL.
- Perform the cyclization reaction by incubating the sample in a table shaker at 800 rpm and 37 °C for 48 hours.

3.2.7 Quality control

3.2.7.1 Mass spectrometry

The overall quality of [6P4]CCL5, disulfide bond formation as well as efficiency of N-terminal glutamine cyclization may be assessed by ESI-TOF MS involving the following steps:

- Wash a C4 MicroSpin column with 100 µL pure ACN for 1 min at 500 *g* in a tabletop centrifuge.
- Add 100 µL H_2O and wash the column by centrifuging for 1 min at 500 *g*. Repeat this step twice.
- Apply sample (2–200 µL) to the column, e.g., 50 µL 0.2 mg/mL protein in MS buffer A for 1 min at 500 *g*.
- Wash the column twice with 50 µL of MS buffer A for 1 min at 500 *g*.
- Elute with 50 µL of MS buffer B for 2 min at 500 *g*.
- Apply eluate to ESI-TOF mass spectrometer.

Figure 3C shows representative examples of the MS characterization of [6P4]CCL5 before (top) and after N-terminal cyclization (bottom). The corresponding masses confirm the protein integrity and completeness of the cyclization step.

3.2.7.2 NMR spectroscopy

Alternatively, the quality of the produced chemokine and the N-terminal cyclization can be assayed at high resolution by NMR spectroscopy. For this, the chemokine analog is expressed in minimal medium containing ^{15}N-labeled ammonium chloride as the sole nitrogen source. A typical NMR sample is then prepared as a 270-µL volume of 100–200 µM ^{15}N-labeled chemokine in suitable buffer and placed in a Shigemi microtube, followed by measurement of a ^{1}H-^{15}N HSQC spectrum.

An example of a [6P4]CCL5 ^{1}H-^{15}N HSQC is shown in Figure 4D. [6P4]CCL5 exhibits well-dispersed ^{1}H-^{15}N backbone amide resonances characteristic of a folded protein containing β-sheets. The ^{1}H-^{15}N resonances are labeled by the respective assigned amino acids. Cyclization of Q0 results in a shift of the glycine 1 (G1) resonance from its non-cyclized (n) to its cyclized (c) form. The

extent of cyclization can be quantified from the ratio of cyclized to non-cyclized G1 resonance intensities.

3.3 Chemokine receptor expression and membrane preparation

A schematic overview of the CCR5 chemokine receptor expression and purification is shown on the left side of Figure 2. CCR5 is expressed in baculovirus-infected insect cells (Smith et al., 1983) using the Invitrogen Bac-to-Bac system for the generation of the recombinant virus and Sf9 cells for expression. A step-by-step protocol for the virus production and insect cell expression can be found in the manufacturer's manual (https://tools.thermofisher.com/content/sfs/manuals/bactobac_man.pdf). The expression is followed by membrane preparation, solubilization, purification and complex formation steps. As the procedures are lengthy, it is most practical to first prepare frozen receptor membranes, and then proceed to the following steps as time permits.

3.3.1 Equipment and materials

- Temperature-controlled incubator shaker (Infors, HT Multitron)
- Bioreactor tubes (TPP, TubeSpin)
- 5-L plastic bottle for insect cells (VWR, 215-1435)
- Breathable rayon film (VWR, 391-1262)
- Automated cell counter (Invitrogen, Countess)
- Cell counting slides (Eve)
- Flow cytometer (Orflo, Moxi Flow)
- Flow cytometer cassettes (Orflo, Moxi Flow Type MF-F)
- SDS-PAGE system (Bio-Rad)
- Precast 4–20% gradient SDS-PAGE gels (Bio-Rad)
- Blotting system for western blot (Bio-Rad, Trans-Blot turbo)
- Western blot transfer packs (Bio-Rad, Trans-Blot turbo mini)
- Electric dispenser (IKA, ULTRA-TURRAX T25)
- Tabletop centrifuge (Eppendorf, 5430 R)
- Ultracentrifuge (Beckman Coulter, Optima XE)

3.3.2 Reagents

- *Spodoptera frugiperda* Sf9 cells (Oxford Expression Technologies)
- Insect cell culture medium (BioConcept, SF-4 baculo express ICM)
- Trypan blue
- Sodium chloride
- Potassium chloride

- Magnesium chloride
- 4-(2-hydroxyethyl)-1-piperazineethanesulfonic acid (HEPES)
- Glycerol
- EDTA-free protease inhibitor tablets (Roche, cOmplete)
- FuGENE transfection reagent (Promega)
- Phycoerythrin (PE)-conjugated 2D7 CCR5-specific conformation-dependent antibody (BD Biosciences, PE mouse anti-human CD195, clone 2D7/CCR5)
- Monoclonal anti-DYKDDDK (anti-FLAG)-peroxidase antibody (Sigma-Aldrich, ANTI-FLAG M2-Peroxidase)
- PE-conjugated anti-baculovirus envelope gp64 antibody (Invitrogen)

3.3.3 Buffers

- Lysis buffer: 10 mM HEPES, 10 mM $MgCl_2$, 20 mM KCl, pH 7.5
- High-salt buffer: 10 mM HEPES, 10 mM $MgCl_2$, 20 mM KCl, 1 M NaCl, pH 7.5
- Freezing buffer: 10 mM HEPES, 10 mM $MgCl_2$, 20 mM KCl, 30% glycerol, pH 7.5
- Phosphate-buffered saline pH 7.4 (PBS; Gibco)

3.3.4 DNA construct

To allow for the detection by western blot and purification by an M2 anti-FLAG resin, the full-length wild-type CCR5 sequence was extended by a C-terminal PreScission protease cleavage site and a FLAG tag. This construct was cloned into a pFastBac1 vector (Invitrogen), which is under the control of the polH promoter. The full protein sequence including the C-terminal extension (CCR5 in bold) is:

MDYQVSSPIYDINYYTSEPCQKINVKQIAARLLPPLYSLVFIFGFVGNMLVILILINCKRLKS
MTDIYLLNLAISDLFFLLTVPFWAHYAAAQWDFGNTMCQLLTGLYFIGFFSGIFFIILLTIDR
YLAVVHAVFALKARTVTFGVVTSVITWVVAVFASLPGIIFTRSQKEGLHYTCSSHFPYSQYQF
WKNFQTLKIVILGLVLPLLVMVICYSGILKTLLRCRNEKKRHRAVRLIFTIMIVYFLFWAPYN
IVLLLNTFQEFFGLNNCSSSNRLDQAMQVTETLGMTHCCINPIIYAFVGEKFRNYLLVFFQKH
IAKRFCKCCSIFQQEAPERASSVYTRSTGEQEISVGLGVAGLEVLFQGPDYKDDDDK

3.3.5 Expression and membrane preparation

- Produce recombinant P2 baculovirus stock according to the Bac-to-Bac protocol and store the virus at 4 °C. Use relatively fresh P2 virus (not older than 1 month) for all following steps.

3.3.5.1 Monitoring of insect cell parameters

Many of the following steps include monitoring of the insect cell parameters size, viability and cell density. The procedure is as follows:

- Take an aliquot of 10 µL cell culture and stain with 10 µL of trypan blue.
- Apply 10 µL of the stained cells to the cell counting slide of the automated cell counter and determine the cell parameters.

3.3.5.2 Determination of optimal virus titer

The following describes small-scale test expressions at several virus dilutions to determine the optimal P2 virus titer for protein expression.

- Test the cell culture for the cell parameters.
- Prepare six 50-mL bioreactor test tubes containing each 20 mL of cell culture at a cell density of 2.5–3.0 10^6 cells/mL.

- Add virus to the test tubes to reach final concentrations of 0, 2, 5, 10, 20 and 40 mL virus solution per liter cell culture.
- At 6 hours post infection (hpi), take 100 µL from each test tube and determine the fraction of infected cells by flow cytometry as follows
    - Centrifuge the 100 µL in a tabletop centrifuge at 1500 *g* for 1 min.
    - Discard the supernatant, add 100 µL PBS and centrifuge again for 1 min (repeat this step twice).
    - Resuspend the cell pellet in 100 µL PBS and add 0.5 µL of 0.2 µg/µL PE-conjugated anti-baculovirus envelope gp64 antibody. Incubate for 15 min in the dark.
    - Centrifuge in a tabletop centrifuge at 1500 *g* for 1 min, discard the supernatant and resuspend the pellet by adding 100 µL PBS. Repeat this step twice.
    - Inject 75 µL into the fill port of the flow cytometer cassette. Adjust the gating of the flow cytometer to separate infected, non-infected and dead cells.
- The optimal virus titer is the minimal amount of P2 virus at which at least 90% of the cells are infected. In our hands, the optimal P2 titer was 10 mL virus per liter cell culture.
- Continue maintaining the remainder of the test culture, which has the optimal P2 virus titer, to determine the optimal harvest time in the subsequent steps.

3.3.5.3 Determination of optimal harvest time

To determine the optimal harvest time, monitor the continued culture by measuring cell parameters and taking samples for western blot at 24, 42, 44, 46 and 48 hpi.

- The cell size normally increases by 20-25% at 24 hpi, while the viability remains at about 98%. At 40–48 hpi, the viability usually drops to 85–90%.
- At 24 hpi and at about 40–46 hpi, i.e. ~85-90% viability, test the appearance level of correctly folded CCR5 at the insect surface by flow cytometry using the PE-conjugated 2D7 conformation-dependent CCR5 antibody. Include a negative control (e.g., uninfected cells) together with the samples.
- To determine the CCR5 expression levels during the time course, analyze the previously taken samples on SDS-PAGE followed by western blot with the anti-FLAG-peroxidase antibody.

The harvesting time is optimal when the viability drops to about 85% and the expression according to the western blot reaches the highest level. In our case this occurred at 46 hpi with more than 95% of the cells showing correctly folded CCR5 at their surface as indicated by the 2D7 antibody. We noted that longer expression times lead to unwanted receptor oligomerization.

3.3.5.4 Large-scale expression

- Inoculate 3 L of *Sf9* insect cells in a 5-L culture bottle with orbital shaking at 27 °C and 130 rpm (25 cm orbit).
- Infect the cells at a cell density of 2.5–3.0 million cells/mL by adding P2 virus at the determined optimal virus titer.
- At 42–46 hpi, confirm that more than 90% of the infected cells are expressing properly folded CCR5 by flow cytometry using the PE-conjugated 2D7 CCR5-specific conformation-dependent antibody.
- Measure the cell viability and cell concentration at the determined optimal harvesting time (the viability should be about 85–90%). Harvest the cells by centrifuging at 1500 *g* for 15 min.
- Freeze the cell pellets in liquid nitrogen and store at -80 °C, or continue directly to membrane preparation.

3.3.5.5 Membrane preparation

- Resuspend the cell pellet from 1 L of Sf-9 cells in 15 mL of lysis buffer.
- Add a protease inhibitor cocktail tablet and homogenize with an electric dispenser.
- Transfer the suspension to an ultracentrifuge tube. Centrifuge at 120,000 *g* for 1 hour, discard the supernatant and resuspend in ~15 mL high-salt buffer. Repeat the process three times with high-salt buffer and then once with lysis buffer.
- Resuspend the pellet in freezing buffer supplemented by a protease inhibitor cocktail tablet to a final volume of 15 mL. Freeze the suspension in liquid nitrogen and store at -80 ˚C until further use.

3.4 Chemokine receptor purification and complex formation

The following describes the purification of CCR5 from 1 L of Sf9 cell culture and the subsequent formation of the receptor complex. In our hands, this protocol yields 0.2 mg of pure receptor per liter of cell culture. For more extensive screening of grid freezing conditions (~27 grids, see below), the preparation is scaled up to processing at least 3 L cell culture. All purification steps are performed on ice or at 4 °C.

3.4.1 Equipment and materials

- Analytical protein liquid chromatography system equipped with autosampler, fraction collector, UV/VIS absorbance and fluorescence detectors (Thermo Fisher Scientific, Ultimate 3000)
- Gel filtration column (Cytiva, Superdex 200 Increase 10/300)
- SDS-PAGE system (Bio-Rad)
- Precast 4–20% gradient SDS-PAGE gels (Bio-Rad)
- Dounce homogenizer (Kontes)
- Ultracentrifuge (Beckman Coulter, Optima XE)
- Tabletop centrifuge (Eppendorf, 5430 R)
- Centrifugal filter unit with ultracel-100 membrane (Amicon Ultra-0.5 and Ultra-4)
- Microvolume spectrophotometer (Thermo Fisher Scientific, NanoDrop)

3.4.2 Reagents

- Iodoacetamide
- Sodium chloride
- Potassium chloride

- Magnesium chloride
- 4-(2-hydroxyethyl)-1-piperazineethanesulfonic acid (HEPES)
- Glycerol
- Dithiothreitol
- Lauryl maltose neopentyl glycol (LMNG)
- Adenosine 5'-triphosphate (ATP)
- Guanosine 5′-*O*-(3′-thiotriphosphate) (GTPγS)
- EDTA-free protease inhibitor tablets (Roche cOmplete)
- Anti-FLAG M2 resin (Sigma-Aldrich)
- Apyrase (NEB)
- Purified human $G\alpha i_1$ subunit from *E. coli* expression (Sun et al., 2015) in $G\alpha_i$ buffer
- Purified bovine transducin $\beta_1\gamma_1$ subunit (Gβγt) from bovine retina (Maeda et al., 2014) in Gβγ buffer
- Purified Fab16 from hybridoma cell culture secreting IgG16 (Tsai et al., 2019) in Fab16 buffer

3.4.3 Buffers

- Lysis buffer: 10 mM HEPES, 10 mM $MgCl_2$, 20 mM KCl, pH 7.5
- 2x solubilization buffer: 100 mM HEPES, 800 mM NaCl, 1% LMNG (prepared from 5% (w/v) stock), pH 7.5
- FLAG binding buffer: 25 mM HEPES, 400 mM NaCl, 10% glycerol, 0.01% LMNG, pH 7.5
- FLAG wash buffer: 25 mM HEPES, 400 mM NaCl, 10% glycerol, 0.01% LMNG, 5 mM ATP, 10 mM $MgCl_2$, pH 7.5
- FLAG elution buffer: 25 mM HEPES, 400 mM NaCl, 10% glycerol, 0.01% LMNG, 0.2 mg/mL FLAG peptide, pH 7.5
- Size-exclusion chromatography (SEC) buffer: 25 mM HEPES, 150 mM NaCl, 0.01% LMNG, pH 7.5
- $G\alpha_i$ buffer: 25 mM HEPES, 2 mM dithiothreitol, 150 mM NaCl, 20% glycerol, pH 7.5
- Gβγ buffer: 10 mM HEPES, 4 mM $MgCl_2$, 2 mM dithiothreitol, 150 mM NaCl, 30% glycerol, pH 7.5
- Fab16 buffer: PBS, 1.5 mM NaN_3, 10% glycerol, pH 7.4

3.4.4 Receptor purification

- Thaw the membranes from 1 L of cell culture and add lysis buffer to a final volume of 25 mL, together with 1 tablet of EDTA-free protein inhibitor cocktail and 2 mg/mL iodoacetamide. Dounce homogenize with 20 strokes and incubate for 1 hour on a rotisserie.
- Add 25 mL of 2x solubilization buffer to the homogenized sample and incubate for 3 hours under gentle mixing on the rotisserie. Centrifuge the solubilized sample at 140,000 *g* for 1 hour.

- Transfer the supernatant to a new reaction tube and add 1 mL of equilibrated anti-FLAG M2 affinity resin. Incubate overnight under gentle mixing on the rotisserie.
- Transfer the resin to an open glass column to collect the resin. Wash the resin consecutively with 10 CV FLAG binding buffer, 10 CV FLAG wash buffer, and 6 CV FLAG binding buffer.
- Remove the flow-through and add 4-5 CV FLAG elution buffer to the resin. Incubate for 15 min and collect the eluate.
- Determine the receptor concentration from A_{280} using the microvolume photometer and analyze the receptor by SDS-PAGE to estimate its purity. Adjust the final receptor concentration to 0.2–0.3 mg/mL in FLAG binding buffer.

3.4.5 Receptor complex formation

The following describes the formation of the [6P4]CCL5•CCR5•G_i complex in the absence and presence of the antibody fragment Fab16, which had been shown to stabilize other GPCR/G protein complexes by recognizing an interface between Gα and Gβγ subunits in the heterotrimer, and to confer resistance to GTPγS-triggered dissociation (Maeda et al., 2018). As it was initially unclear whether Fab16 would also stabilize the [6P4]CCL5•CCR5•G_i complex, a respective assay was carried out (see below), which indicated significant stabilization also for this complex. In consequence, we proceeded to the full cryo-EM analysis only with the [6P4]CCL5•CCR5•G_i•Fab16 complex.

- Form the G_i protein heterotrimer by incubating 50 µL 10 mg/mL $G\alpha_i$ in $G\alpha_i$ buffer with 250 µL 2.5 mg/mL Gβγ in Gβγ buffer for 30 min on ice.
- Add the formed G_i protein heterotrimer to 4 mL 0.2 mg/mL (~2–3 µM monomeric) CCR5 eluted from the FLAG resin and incubate for 30 min.
- Add 90 µL 1 mg/mL cyclized [6P4]CCL5 to the preformed complex to reach a 1:1 stoichiometric ratio with CCR5, i.e. a final concentration of ~2–3 µM. Supplement the mixture with 25 mU/mL apyrase which hydrolyzes nucleotides in order to obtain the nucleotide-free complex. Incubate the

complex for 2 hours under gentle rotation. Keep 500 µL of the formed [6P4]CCL5•CCR5•G_i complex for further use.

- Add 800 µL 0.8 mg/mL Fab16 to the remaining complex solution, and incubate for 1 hour under gentle rotation.
- Concentrate the [6P4]CCL5•CCR5•G_i•Fab16 complex to 400–600 µL using a concentrator with 100 kDa MWCO. Spin the sample at 20,000 *g* for 10 min to remove any precipitate.
- Estimate the concentrations of both complexes from A_{280} using the microvolume photometer and take aliquots for SDS-PAGE analysis.

3.4.6 Receptor complex purification

- Connect the Superdex 200 Increase 10/300 gel filtration column to a liquid chromatography (HPLC or FPLC) system equipped with a UV absorbance detector, autosampler and fraction collector. Equilibrate the column with 2 CV of SEC buffer at a flow rate of 0.5 mL/min.
- Perform a SEC program, which sequentially injects the receptor complex solution to the column, applies 1 CV of SEC buffer at 0.5 mL/min, monitors the absorbance at 280 nm, and collects 150-µL fractions in a 96-well plate fraction collector.
- Determine A_{280} of the fractions with a microvolume spectrophotometer to estimate the receptor complex concentration.
- Analyze the SEC fractions and the individual complex components as standards by SDS-PAGE.
- Combine the fractions showing good purity and complex integrity and concentrate them for further use.

Figures 4A, B (left) show representative SEC profiles of the complexes without and with Fab16, respectively. A significant part of the complex contains oligomers and higher molecular weight impurities. However, these impurities were successfully separated from the main complexes, which elute at 10.9 mL for the complex without Fab16 and at 10.5 mL with Fab16. The SDS-PAGE analyses of both complexes are shown on the right side of Figures 4A, B. The

fractions which were taken for the cryo-EM grid preparation are delimited by orange dashed lines.

3.5 Quality control of receptor complex stability by GTPγS binding assay

While the cryo-EM grids should be prepared immediately after complex formation (see below), the following test can be performed to assess the specificity and stability of the formed [6P4]CCL5•CCR5•G_i complex and the effect of Fab16. The test is based on the GTPγS-triggered dissociation of the G_i heterotrimer, which is followed by analytical fluorescence-detection size-exclusion chromatography (FSEC) using the intrinsic tryptophan fluorescence. As standards also the individual complex components are analyzed by FSEC. All steps are performed on ice or at 4 °C

- Prepare the following standards at concentrations of ~0.1–0.3 mg/mL and volumes of 110 µL in SEC buffer for FSEC analysis:
    - $G\alpha_i$
    - Gβγ
    - Fab16
    - G_i heterotrimer formed from $G\alpha_i$, Gβγ mixture incubated for 1 hour
    - G_i heterotrimer•Fab16 complex formed from $G\alpha_i$, Gβγ, Fab16 mixture incubated for 1 hour
- Dilute the SEC-purified [6P4]CCL5•CCR5•G_i and [6P4]CCL5•CCR5•G_i•Fab16 complexes to ~0.1 mg/mL and 220-µL volumes. Split each complex solution into two equal portions, add 100 µM GTPγS (10 mM stock solution) to one part, and incubate for 1 hour.
- Transfer all samples to glass vials and place them in the autosampler connected to the HPLC system with the Superdex 200 Increase 10/300 gel filtration column.
- Set up a program for the SEC run, which sequentially injects 80 µL of the samples to the column, then applies 1 CV of SEC buffer at a flow rate of 0.4 mL/min, and monitors the protein tryptophan fluorescence (λ_{ex} = 280 nm; λ_{em} = 380 nm).

Figure 4C shows representative chromatograms of this stability analysis. The [6P4]CCL5•CCR5•G_i complex (red) dissociates in the presence of GTPγS (dark blue). Similar to other GPCR/G protein complexes (Maeda et al., 2018), the addition of Fab16 (orange) was found to stabilize the CCR5/G_i complex in the presence of GTPγS (light blue).

3.6 Preparation of cryo-EM grids

The grids for cryo-EM analysis should be prepared immediately from the freshly purified complex. The following gives a short overview of the preparation. More detailed protocols can be found elsewhere (Goldie et al., 2014).

3.6.1 Equipment and materials

- Glow Discharge system for EM grids (Quorum, GloQube)
- EM grids (Quantifoil, R1.2/1.3 200-mesh copper)
- Plunge freezer (Thermo Fisher Scientific, Vitrobot Mark IV)
- Cryogen cup (Thermo Fisher Scientific, Vitrobot)
- Filter paper (Thermo Fisher Scientific, Standard Vitrobot filter paper, 55/20 mm, Grade 595)
- 60-mL syringe
- Tweezers for EM grid handling (e.g., Electron Microscopy Sciences, Dumont #7)
- Cryo grid boxes with lid (Agar Scientific)
- Cryo Dewar
- Liquid nitrogen
- Ethane gas

3.6.2 Cryo-EM grid preparation

- Prepare liquid ethane from ethane gas using the assembled cryogen cup cooled with liquid nitrogen.
- Glow discharge EM grids at 25 mA for 30 sec using the glow discharge system.

- Set the humidity to 100% and the temperature to 4 °C on the Vitrobot plunge freezer.
- Prepare purified complex samples at various concentrations ranging from 1 to 5 mg/mL (Table 1), either by concentrating in a centrifugal filter unit with a 100-kDa MWCO or diluting in SEC buffer.
- Load 3.5 µL of the purified complex at the various concentrations to the carbon-coated side of the glow-discharged EM grid.
- Remove excess liquid on the grid by blotting with filter paper using various blot forces and time periods (Table 1) with triplicates for each condition to optimize ice thickness.
- Plunge the blot-dried grid into cooled liquid ethane (~ -180 °C) for rapid freezing in order to form a thin layer of amorphous ice.
- Transfer prepared grids to liquid nitrogen in a cryo Dewar for storage until use for cryo-EM analysis.

4 Discussion and Conclusion

The structure determination of chemokine-chemokine receptor complexes has long been challenging due to difficulties in obtaining highly purified chemokine receptors, the intrinsic tendencies of chemokines, receptors and their complexes to aggregate, heterogeneity and low stability of the complexes, and their intrinsic mobility. This chapter provides detailed protocols for the production of the superagonist [6P4]CCL5 chemokine variant and for its cognate receptor CCR5 in wild-type form, as well as for the formation of their complex with the G_i heterotrimer and the stabilizing Fab16 antibody fragment, which lead to the successful cryo-EM structure determination of the [6P4]CCL5•CCR5•G_i complex.

In the current procedure, the individual complex components are prepared separately and then combined to form the complex. For proper interaction with CCR5, it is essential to obtain the CCL5 chemokine with a native N-terminus devoid of any further residues from cloning or *E. coli* expression. This is achieved by a DNA construct, which encodes CCL5 with a cleavable N-terminal thioredoxin

His-tag fusion. After expression and an unfolding-reduction, reoxidation-refolding purification sequence, the fusion is efficiently cleaved by enterokinase to obtain the blunt-ended CCL5 N-terminus. In the specific case of [6P4]CCL5, the N-terminal glutamine then spontaneously cyclizes to form pyroglutamate. The protocol achieves a robust yield of ~10 mg pure and homogeneous [6P4]CCL5 from 1 liter of bacterial culture. The high quality of the purified chemokine can be assayed by mass spectrometry and NMR analysis. Other chemokines and their analogs may be obtained in a similar manner. Despite a certain tendency of [6P4]CCL5 to aggregate, a sufficient amount of monomeric [6P4]CCL5•CCR5•G_i for the cryo-EM analysis was obtained. However, other chemokines, such as native CCL5, may even be more prone to aggregation, which presents additional challenges.

The aggregation problem is compounded by the tendency of the chemokine receptors themselves to aggregate. In the present case, the expression of the full-length, wild-type CCR5 in insect cells yielded a mixture of CCR5 monomers, dimers and higher oligomers, which in our hands was considerably more heterogeneous than the expression product of a CCR5 construct optimized for crystallization of the inactive [5P7]CCL5•CCR5 complex (Zheng et al., 2017). In this respect, we observed that longer CCR5 expression times in the insect cells lead to stronger oligomerization. Thus, it is very important to carefully optimize and control all insect cell expression parameters such as virus titer, harvesting time, level of receptor expression and receptor structural quality. For the latter, recognition by the structure-specific antibody 2D7 was a very useful indicator of properly folded CCR5 on the surface of the insect cells. In addition, the structural integrity and homogeneity of the receptor preparation depends critically on the appropriate detergent. Detailed protocols for detergent screening for GPCRs have been described elsewhere (Pamula et al., 2020). In the present case, as in many others, LMNG proved best due to its high efficiency of CCR5 membrane extraction, its low critical micelle concentration (CMC), and consequently efficient removal by dialysis and lower background in the cryo-EM images.

Despite the heterogeneity of the CCR5 receptor preparation and of the formed [6P4]CCL5•CCR5•G_i complex solution, a reasonably homogeneous

sample was obtained from this after complex formation with the chemokine and the G protein by SEC (Figure 4), which could then be further purified ‘in silico’ during the cryo-EM data analysis. Nevertheless, heterogeneity is clearly limiting all steps, and it was critical to form the complex at low (~2–3 µM) chemokine and receptor concentrations to avoid aggregation as much as possible. This is practical for [6P4]CCL5, which has a low nanomolar affinity for CCR5 (Rico et al., 2019). However, other chemokines such as wild-type CCL5 (Rico et al., 2019) often have weaker affinities for their receptors, which makes complex formation at low micromolar concentrations impossible. An alternative approach to reduce aggregation could be the co-expression of G protein and/or chemokine with the receptor. Co-expression with the G protein may increase the affinity of agonist chemokines and has been successful for the cryo-EM structure determination of a number of other active, non-chemokine GPCR•G protein complexes (Qiao et al., 2020; Xu et al., 2021; Zhuang et al., 2021). Co-expression with the [5P7]CCL5 antagonist chemokine has been used for the X-ray structure determination of the [5P7]CCL5•CCR5 complex (Zheng et al., 2017). Again, however, these approaches depend on a sufficient affinity of the chemokine for the receptor (Gustavsson et al., 2016).

In summary, with the advances in cryo-EM technology and in the production of chemokine receptors, chemokines and G proteins, the structure determination and in-depth biophysical characterization of many further chemokine•receptor•G protein complexes seems in reach. This is a prerequisite for deciphering the complex interactions of the components of the chemokine signaling system and to move forward in the rational drug design against these important therapeutic targets.

5 Tables

Table 1. Cryo-EM grid plunge-freezing conditions

Receptor complex concentration [mg/mL]	**Blot force [Vitrobot units]**	**Blot time [s]**
1	20	2
	10	3
	20	3
2.5	20	2
	10	3
	20	3
5	20	2
	10	3
	20	3

6 Figure Legends

Figure 1. Overview of currently available chemokine•chemokine receptor complex structures. Receptors in their active and inactive conformation are colored in green and blue, respectively. Only CCR5 has been solved in both active, agonist- and inactive, antagonist-bound states. Chemokines are shown in magenta, intracellular binding partners in orange, and stabilizing intra-receptor fusion proteins in grey. CCR5 complexes marked with asterisks were expressed as chemokine-chemokine receptor fusion proteins.

Figure 2. Overall scheme of the [6P4]CCL5•CCR5•G_i•Fab16 complex preparation for cryo-EM studies.

Figure 3. Chemokine preparation and characterization. A. [6P4]CCL5 expression construct. B. Production scheme for [6P4]CCL5 chemokine cyclized at its N-terminal glutamine Q0 to pyroglutamate and controls by SDS-PAGE analysis. C. Mass spectra of purified N-terminally non-cyclized and cyclized [6P4]CCL5. D. ^{1}H-^{15}N HSQC spectrum of [6P4]CCL5 in 25 mM phosphate, 5% D_2O, 0.02% NaN_3, pH 3.8 obtained with acquisition times of 86 ms (^{1}H) and 56 ms (^{15}N) at 600 MHz and 25 °C. The NMR data were processed with the NMRpipe suite of programs (Delaglio et al., 1995) and analyzed using the program NMRFAM-Sparky (Lee et al., 2015). As Q0 of [6P4]CCL5 was not yet fully cyclized, resonances of both non-cyclized and cyclized molecular species are visible for glycine-1 [G1(n) and G1(c), respectively].

Figure 4. Characterization of the [6P4]CCL5•CCR5•G_i complex. A. Size-exclusion chromatography (SEC) profiles of [6P4]CCL5•CCR5•G_i complex (left) and SDS-PAGE analysis of the SEC fractions (right). The fractions are marked with numbers at the top and are separated by dashed lines in the chromatogram. Orange dashed lines delimit the fractions of the complex. B. Same analysis as A for the [6P4]CCL5•CCR5•G_i•Fab16 complex. C. Superimposed FSEC profiles of the [6P4]CCL5•CCR5•G_i complex with and without added Fab16 in presence of GTPγS. The FSEC profiles of the individual complex components are shown as controls. The [6P4]CCL5•CCR5•G_i complex (red) disintegrates partially in the presence of GTPγS (dark blue). The stability of the complex in the presence of

GTPγS (light blue) is increased upon addition of Fab16 (orange), as the antibody fragment constrains the conformational flexibility of the G_i heterotrimer.

7 Acknowledgments

This work was supported by the Swiss National Science Foundation (Grants 31-201270 and IZLIZ3-200298 to S.G.). We thank Prof. P. LiWang (UC Merced) for the gift of the [5P14]CCL5 DNA construct, J. Mühle (Paul Scherrer Institute, Villigen) for preparation of the Fab16, Philip Pamula (Paul Scherrer Institute, Villigen) for preparation of the G_i protein, and Prof. G. Schertler (Paul Scherrer Institute, Villigen) and Prof. O. Hartley (U. Geneva) for helpful discussions.

8 Conflict of Interest

The authors declare no conflict of interest.

9 References

Aldinucci, D., Borghese, C., Casagrande, N., 2020. The CCL5/CCR5 Axis in Cancer Progression. Cancers 12, 1765. https://doi.org/10.3390/cancers12071765

Aldinucci, D., Casagrande, N., 2018. Inhibition of the CCL5/CCR5 Axis against the Progression of Gastric Cancer. International Journal of Molecular Sciences 19, 1477. https://doi.org/10.3390/ijms19051477

Alkhatib, G., 2009. The biology of CCR5 and CXCR4: Current Opinion in HIV and AIDS 4, 96–103. https://doi.org/10.1097/COH.0b013e328324bbec

Apel, A.-K., Cheng, R.K.Y., Tautermann, C.S., Brauchle, M., Huang, C.-Y., Pautsch, A., Hennig, M., Nar, H., Schnapp, G., 2019. Crystal Structure of CC Chemokine Receptor 2A in Complex with an Orthosteric Antagonist Provides Insights for the Design of Selective Antagonists. Structure 27, 427-438.e5. https://doi.org/10.1016/j.str.2018.10.027

Bachelerie, F., Ben-Baruch, A., Burkhardt, A.M., Combadiere, C., Farber, J.M., Graham, G.J., Horuk, R., Sparre-Ulrich, A.H., Locati, M., Luster, A.D., Mantovani, A., Matsushima, K., Murphy, P.M., Nibbs, R., Nomiyama, H., Power, C.A., Proudfoot, A.E.I., Rosenkilde, M.M., Rot, A., Sozzani, S., Thelen, M., Yoshie, O., Zlotnik, A., 2014. International Union of Basic and Clinical Pharmacology. LXXXIX. Update on the Extended Family of Chemokine Receptors and Introducing a New Nomenclature for Atypical Chemokine Receptors. Pharmacol Rev 66, 1–79. https://doi.org/10.1124/pr.113.007724

Brelot, A., Chakrabarti, L.A., 2018. CCR5 Revisited: How Mechanisms of HIV Entry Govern AIDS Pathogenesis. Journal of Molecular Biology 430, 2557–2589. https://doi.org/10.1016/j.jmb.2018.06.027

Burg, J.S., Ingram, J.R., Venkatakrishnan, A.J., Jude, K.M., Dukkipati, A., Feinberg, E.N., Angelini, A., Waghray, D., Dror, R.O., Ploegh, H.L., Garcia, K.C., 2015. Structural basis for chemokine recognition and activation of a viral G protein-coupled receptor. Science 347, 1113–1117. https://doi.org/10.1126/science.aaa5026

Cai, M., Huang, Y., Sakaguchi, K., Clore, G.M., Gronenborn, A.M., Craigie, R., 1998. An efficient and cost-effective isotope labeling protocol for proteins expressed in Escherichia coli. J Biomol NMR 11, 97–102. https://doi.org/10.1023/a:1008222131470

Chen, Y.-C., Chen, S.-P., Li, J.-Y., Chen, P.-C., Lee, Y.-Z., Li, K.-M., Zarivach, R., Sun, Y.-J., Sue, S.-C., 2020. Integrative Model to Coordinate the Oligomerization and Aggregation Mechanisms of CCL5. Journal of Molecular Biology 432, 1143–1157. https://doi.org/10.1016/j.jmb.2019.12.049

Chua, R.L., Lukassen, S., Trump, S., Hennig, B.P., Wendisch, D., Pott, F., Debnath, O., Thürmann, L., Kurth, F., Völker, M.T., Kazmierski, J., Timmermann, B., Twardziok, S., Schneider, S., Machleidt, F., Müller-Redetzky, H., Maier, M., Krannich, A., Schmidt, S., Balzer, F., Liebig, J., Loske, J., Suttorp, N., Eils, J., Ishaque, N., Liebert, U.G., von Kalle, C., Hocke, A., Witzenrath, M., Goffinet, C., Drosten, C., Laudi, S., Lehmann, I., Conrad, C., Sander, L.-E., Eils, R., 2020. COVID-19 severity correlates with airway epithelium–immune cell interactions identified by single-cell analysis. Nat Biotechnol 38, 970–979. https://doi.org/10.1038/s41587-020-0602-4

Combadiere, C., Ahuja, S.K., Lee Tiffany, H., Murphy, P.M., 1996. Cloning and functional expression of CC CKR5, a human monocyte CC chemokine receptor selective for MIP-1α, MIP-1β, and RANTES. Journal of Leukocyte Biology 60, 147–152. https://doi.org/10.1002/jlb.60.1.147

D'Agostino, G., García-Cuesta, E.M., Gomariz, R.P., Rodríguez-Frade, J.M., Mellado, M., 2020. The multilayered complexity of the chemokine receptor system. Biochemical and Biophysical Research Communications 528, 347–358. https://doi.org/10.1016/j.bbrc.2020.02.120

Delaglio, F., Grzesiek, S., Vuister, G.W., Zhu, G., Pfeifer, J., Bax, A., 1995. NMRPipe: A multidimensional spectral processing system based on UNIX pipes. J Biomol NMR 6, 277–293. https://doi.org/10.1007/BF00197809

Duma, L., Häussinger, D., Rogowski, M., Lusso, P., Grzesiek, S., 2007. Recognition of RANTES by Extracellular Parts of the CCR5 Receptor. Journal of Molecular Biology 365, 1063–1075. https://doi.org/10.1016/j.jmb.2006.10.040

Fernando, H., Chin, C., Rösgen, J., Rajarathnam, K., 2004. Dimer Dissociation Is Essential for Interleukin-8 (IL-8) Binding to CXCR1 Receptor*. Journal of Biological Chemistry 279, 36175–36178. https://doi.org/10.1074/jbc.C400283200

Gaertner, H., Cerini, F., Escola, J.M., Kuenzi, G., Melotti, A., Offord, R., Rossitto-Borlat, I., Nedellec, R., Salkowitz, J., Gorochov, G., Mosier, D., Hartley, O., 2008. Highly potent, fully recombinant anti-HIV chemokines: Reengineering a low-cost microbicide. Proceedings Of The National Academy Of Sciences Of The United States Of America 105, 17706–17711. https://doi.org/10.1073/pnas.0805098105

Goldie, K.N., Abeyrathne, P., Kebbel, F., Chami, M., Ringler, P., Stahlberg, H., 2014. Cryo-electron Microscopy of Membrane Proteins, in: Kuo, J. (Ed.), Electron Microscopy: Methods and Protocols, Methods in Molecular Biology. Humana Press, Totowa, NJ, pp. 325–341. https://doi.org/10.1007/978-1-62703-776-1_15

Gustavsson, M., Zheng, Y., Handel, T.M., 2016. Production of chemokine/chemokine receptor complexes for structural and biophysical studies. Methods Enzymol 570, 233–260. https://doi.org/10.1016/bs.mie.2015.10.003

Handel, T.M., Dyer, D.P., 2021. Perspectives on the Biological Role of Chemokine:Glycosaminoglycan Interactions. J Histochem Cytochem. 69, 87–91. https://doi.org/10.1369/0022155420977971

Isaikina, P., Tsai, C.-J., Dietz, N., Pamula, F., Grahl, A., Goldie, K.N., Guixà-González, R., Branco, C., Paolini-Bertrand, M., Calo, N., Cerini, F., Schertler, G.F.X., Hartley, O., Stahlberg, H., Maier, T., Deupi, X., Grzesiek, S., 2021. Structural basis of the activation of the CC chemokine receptor 5 by a chemokine agonist. Science Advances 7, eabg8685. https://doi.org/10.1126/sciadv.abg8685

Jaeger, K., Bruenle, S., Weinert, T., Guba, W., Muehle, J., Miyazaki, T., Weber, M., Furrer, A., Haenggi, N., Tetaz, T., Huang, C.-Y., Mattle, D., Vonach, J.-M., Gast, A., Kuglstatter, A., Rudolph, M.G., Nogly, P., Benz, J., Dawson, R.J.P., Standfuss, J., 2019. Structural Basis for Allosteric Ligand Recognition in the Human CC Chemokine Receptor 7. Cell 178, 1222-1230.e10. https://doi.org/10.1016/j.cell.2019.07.028

Kessler, N., Akabayov, S.R., Moseri, A., Cohen, L.S., Sakhapov, D., Bolton, D., Fridman, B., Kay, L.E., Naider, F., Anglister, J., 2020. Allovalency observed by transferred NOE: interactions of sulfated tyrosine residues in the N-terminal segment of CCR5 with the CCL5 chemokine. The FEBS Journal doi: 10.1111/febs.15503. Online ahead of print. https://doi.org/10.1111/febs.15503

Kraus, S., Kolman, T., Yeung, A., Deming, D., 2021. Chemokine Receptor Antagonists: Role in Oncology. Curr Oncol Rep 23, 131. https://doi.org/10.1007/s11912-021-01117-8

Lai, W.Y., Mueller, A., 2021. Latest update on chemokine receptors as therapeutic targets. Biochemical Society Transactions 49, 1385–1395. https://doi.org/10.1042/BST20201114

Lee, W., Tonelli, M., Markley, J.L., 2015. NMRFAM-SPARKY: enhanced software for biomolecular NMR spectroscopy. Bioinformatics 31, 1325–1327. https://doi.org/10.1093/bioinformatics/btu830

Liu, K., Wu, L., Yuan, S., Wu, M., Xu, Y., Sun, Q., Li, S., Zhao, S., Hua, T., Liu, Z.-J., 2020. Structural basis of CXC chemokine receptor 2 activation and signalling. Nature 585, 135–140. https://doi.org/10.1038/s41586-020-2492-5

Maeda, S., Koehl, A., Matile, H., Hu, H., Hilger, D., Schertler, G.F.X., Manglik, A., Skiniotis, G., Dawson, R.J.P., Kobilka, B.K., 2018. Development of an antibody fragment that stabilizes GPCR/G-protein complexes. Nat Commun 9. https://doi.org/10.1038/s41467-018-06002-w

Maeda, S., Sun, D., Singhal, A., Foggetta, M., Schmid, G., Standfuss, J., Hennig, M., Dawson, R.J.P., Veprintsev, D.B., Schertler, G.F.X., 2014. Crystallization Scale Preparation of a Stable GPCR Signaling Complex between Constitutively Active Rhodopsin and G-Protein. PLOS ONE 9, e98714. https://doi.org/10.1371/journal.pone.0098714

Martin-Blondel, G., Brassat, D., Bauer, J., Lassmann, H., Liblau, R.S., 2016. CCR5 blockade for neuroinflammatory diseases — beyond control of HIV. Nat Rev Neurol 12, 95–105. https://doi.org/10.1038/nrneurol.2015.248

Miles, T.F., Spiess, K., Jude, K.M., Tsutsumi, N., Burg, J.S., Ingram, J.R., Waghray, D., Hjorto, G.M., Larsen, O., Ploegh, H.L., Rosenkilde, M.M., Garcia, K.C., 2018. Viral GPCR US28 can signal in response to chemokine agonists of nearly unlimited structural degeneracy. eLife 7, e35850. https://doi.org/10.7554/eLife.35850

Miller, M.C., Mayo, K.H., 2017. Chemokines from a Structural Perspective. International Journal of Molecular Sciences 18, 2088. https://doi.org/10.3390/ijms18102088

Ortiz Zacarías, N.V., Bemelmans, M.P., Handel, T.M., de Visser, K.E., Heitman, L.H., 2021. Anticancer opportunities at every stage of chemokine function. Trends in Pharmacological Sciences 42, 912–928. https://doi.org/10.1016/j.tips.2021.08.001

Oswald, C., Rappas, M., Kean, J., Doré, A.S., Errey, J.C., Bennett, K., Deflorian, F., Christopher, J.A., Jazayeri, A., Mason, J.S., Congreve, M., Cooke, R.M., Marshall, F.H., 2016. Intracellular allosteric antagonism of the CCR9 receptor. Nature 540, 462–465. https://doi.org/10.1038/nature20606

Pamula, F., Mühle, J., Blanc, A., Nehmé, R., Edwards, P.C., Tate, C.G., Tsai, C.-J., 2020. Strategic Screening and Characterization of the Visual GPCR-mini-G Protein Signaling Complex for Successful Crystallization. JoVE (Journal of Visualized Experiments) e60747. https://doi.org/10.3791/60747

Peng, P., Chen, H., Zhu, Y., Wang, Z., Li, J., Luo, R.-H., Wang, J., Chen, L., Yang, L.-M., Jiang, H., Xie, X., Wu, B., Zheng, Y.-T., Liu, H., 2018. Structure-Based Design of 1-Heteroaryl-1,3-propanediamine Derivatives as a Novel Series of CC-Chemokine Receptor 5 Antagonists. J. Med. Chem. 61, 9621–9636. https://doi.org/10.1021/acs.jmedchem.8b01077

Qiao, A., Han, S., Li, X., Li, Z., Zhao, P., Dai, A., Chang, R., Tai, L., Tan, Q., Chu, X., Ma, L., Thorsen, T.S., Reedtz-Runge, S., Yang, D., Wang, M.-W., Sexton, P.M., Wootten, D., Sun, F., Zhao, Q., Wu, B., 2020. Structural basis of G_s and G_i recognition by the human glucagon receptor. Science 367, 1346–1352. https://doi.org/10.1126/science.aaz5346

Qin, L., Kufareva, I., Holden, L.G., Wang, C., Zheng, Y., Zhao, C., Fenalti, G., Wu, H., Han, G.W., Cherezov, V., Abagyan, R., Stevens, R.C., Handel, T.M., 2015. Structural biology. Crystal structure of the chemokine receptor CXCR4 in complex with a viral chemokine. Science (New York, NY) 347, 1117–1122. https://doi.org/10.1126/science.1261064

Raport, C., Gosling, J., Schweickart, V., Gray, P., Charo, I., 1996. Molecular cloning and functional characterization of a novel human CC chemokine receptor (CCR5) for RANTES, MIP-1beta, and MIP-1alpha. The Journal of biological chemistry 271, 17161–17166.

Ravindran, A., Sawant, K.V., Sarmiento, J., Navarro, J., Rajarathnam, K., 2013. Chemokine CXCL1 Dimer Is a Potent Agonist for the CXCR2 Receptor *. Journal of Biological Chemistry 288, 12244–12252. https://doi.org/10.1074/jbc.M112.443762

Rico, C.A., Berchiche, Y.A., Horioka, M., Peeler, J.C., Lorenzen, E., Tian, H., Kazmi, M.A., Fürstenberg, A., Gaertner, H., Hartley, O., Sakmar, T.P., Huber, T., 2019. High-Affinity Binding of Chemokine Analogs that Display Ligand Bias at the HIV-1 Coreceptor CCR5. Biophysical Journal 117, 903–919. https://doi.org/10.1016/j.bpj.2019.07.043

Samson, M., Labbe, O., Mollereau, C., Vassart, G., Parmentier, M., 1996. Molecular Cloning and Functional Expression of a New Human CC-Chemokine Receptor Gene. Biochemistry 35, 3362–3367. https://doi.org/10.1021/bi952950g

Scurci, I., Martins, E., Hartley, O., 2018. CCR5: Established paradigms and new frontiers for a 'celebrity' chemokine receptor. Cytokine, Special issue: Chemokines - beyond chemotaxis 109, 81–93. https://doi.org/10.1016/j.cyto.2018.02.018

Smith, G.E., Summers, M.D., Fraser, M.J., 1983. Production of human beta interferon in insect cells infected with a baculovirus expression vector. Molecular and cellular biology 3, 2156–2165.

Stone, M.J., Hayward, J.A., Huang, C., E. Huma, Z., Sanchez, J., 2017. Mechanisms of Regulation of the Chemokine-Receptor Network. International Journal of Molecular Sciences 18, 342. https://doi.org/10.3390/ijms18020342

Sun, D., Flock, T., Deupi, X., Maeda, S., Matkovic, M., Mendieta, S., Mayer, D., Dawson, R.J.P., Schertler, G.F.X., Babu, M.M., Veprintsev, D.B., 2015. Probing Gαi1 protein activation at single–amino acid resolution. Nat Struct Mol Biol 22, 686–694. https://doi.org/10.1038/nsmb.3070

Szpakowska, M., Fievez, V., Arumugan, K., van Nuland, N., Schmit, J.-C., Chevigné, A., 2012. Function, diversity and therapeutic potential of the N-terminal domain of human chemokine receptors. Biochemical Pharmacology, REDCAT. Redox regulation: Natural compounds as regulators of inflammation signaling 84, 1366–1380. https://doi.org/10.1016/j.bcp.2012.08.008

Tan, Q., Zhu, Y., Li, J., Chen, Z., Han, G.W., Kufareva, I., Li, T., Ma, L., Fenalti, G., Li, J., Zhang, W., Xie, X., Yang, H., Jiang, H., Cherezov, V., Liu, H., Stevens, R.C., Zhao, Q., Wu, B., 2013. Structure of the CCR5 Chemokine Receptor-HIV Entry Inhibitor Maraviroc Complex. Science 341, 1387–1390. https://doi.org/10.1126/science.1241475

Tsai, C.-J., Marino, J., Adaixo, R., Pamula, F., Muehle, J., Maeda, S., Flock, T., Taylor, N.M., Mohammed, I., Matile, H., Dawson, R.J., Deupi, X., Stahlberg, H., Schertler, G., 2019. Cryo-EM structure of the rhodopsin-Gαi-βγ complex reveals binding of the rhodopsin C-terminal tail to the gβ subunit. eLife 8, e46041. https://doi.org/10.7554/eLife.46041

Wang, X., Watson, C., Sharp, J.S., Handel, T.M., Prestegard, J.H., 2011. Oligomeric Structure of the Chemokine CCL5/RANTES from NMR, MS, and SAXS Data. Structure 19, 1138–1148. https://doi.org/10.1016/j.str.2011.06.001

Wasilko, D.J., Johnson, Z.L., Ammirati, M., Che, Y., Griffor, M.C., Han, S., Wu, H., 2020. Structural basis for chemokine receptor CCR6 activation by the endogenous protein ligand CCL20. Nat Commun 11, 3031. https://doi.org/10.1038/s41467-020-16820-6

Wedemeyer, M.J., Mahn, S.A., Getschman, A.E., Crawford, K.S., Peterson, F.C., Marchese, A., McCorvy, J.D., Volkman, B.F., 2020. The chemokine X-factor: structure-function analysis of the CXC motif at CXCR4 and ACKR3. J. Biol. Chem. jbc.RA120.014244. https://doi.org/10.1074/jbc.RA120.014244

Wiktor, M., Hartley, O., Grzesiek, S., 2013. Characterization of Structure, Dynamics, and Detergent Interactions of the Anti-HIV Chemokine Variant 5P12-RANTES. Biophysical Journal 105, 2586–2597. https://doi.org/10.1016/j.bpj.2013.10.025

Wu, B., Chien, E.Y.T., Mol, C.D., Fenalti, G., Liu, W., Katritch, V., Abagyan, R., Brooun, A., Wells, P., Bi, F.C., Hamel, D.J., Kuhn, P., Handel, T.M., Cherezov, V., Stevens, R.C., 2010. Structures of the CXCR4 Chemokine GPCR with Small-Molecule and Cyclic Peptide Antagonists. Science 330, 1066–1071. https://doi.org/10.1126/science.1194396

Xu, P., Huang, S., Zhang, H., Mao, C., Zhou, X.E., Cheng, X., Simon, I.A., Shen, D.-D., Yen, H.-Y., Robinson, C.V., Harpsøe, K., Svensson, B., Guo, J., Jiang, H., Gloriam, D.E., Melcher, K., Jiang, Y., Zhang, Y., Xu, H.E., 2021. Structural insights into the lipid and ligand regulation of serotonin receptors. Nature 592, 469–473. https://doi.org/10.1038/s41586-021-03376-8

Zhang, H., Chen, K., Tan, Q., Shao, Q., Han, S., Zhang, C., Yi, C., Chu, X., Zhu, Y., Xu, Y., Zhao, Q., Wu, B., 2021. Structural basis for chemokine recognition and receptor activation of chemokine receptor CCR5. Nat Commun 12, 4151. https://doi.org/10.1038/s41467-021-24438-5

Zhao, S., Wu, B., Stevens, R.C., 2019. Advancing Chemokine GPCR Structure Based Drug Discovery. Structure 27, 405–408. https://doi.org/10.1016/j.str.2019.02.004

Zheng, Y., Han, G.W., Abagyan, R., Wu, B., Stevens, R.C., Cherezov, V., Kufareva, I., Handel, T.M., 2017. Structure of CC Chemokine Receptor 5 with a Potent Chemokine Antagonist Reveals Mechanisms of Chemokine Recognition and Molecular Mimicry by HIV. Immunity 46, 1005-1017.e5. https://doi.org/10.1016/j.immuni.2017.05.002

Zheng, Y., Qin, L., Ortiz Zacarías, N.V., de Vries, H., Han, G.W., Gustavsson, M., Dabros, M., Zhao, C., Cherney, R.J., Carter, P., Stamos, D., Abagyan, R., Cherezov, V., Stevens, R.C., IJzerman, A.P., Heitman, L.H., Tebben, A., Kufareva, I., Handel, T.M., 2016. Structure of CC Chemokine Receptor 2 with Orthosteric and Allosteric Antagonists. Nature 540, 458–461. https://doi.org/10.1038/nature20605

Zhuang, Y., Xu, P., Mao, C., Wang, L., Krumm, B., Zhou, X.E., Huang, S., Liu, H., Cheng, X., Huang, X.-P., Shen, D.-D., Xu, T., Liu, Y.-F., Wang, Y., Guo, J., Jiang, Y., Jiang, H., Melcher, K., Roth, B.L., Zhang, Y., Zhang, C., Xu, H.E., 2021. Structural insights into the human D1 and D2 dopamine receptor signaling complexes. Cell 184, 931-942.e18. https://doi.org/10.1016/j.cell.2021.01.027

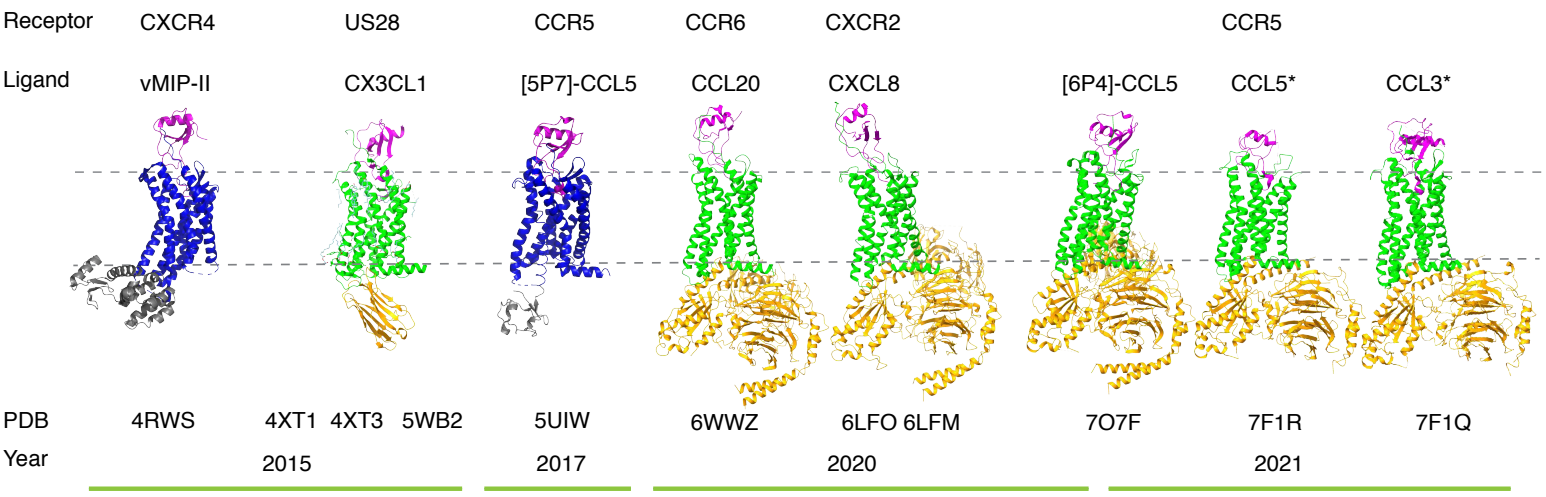
Receptor
CXCR4
US28
CCR5
CCR6
CXCR2
CCR5
Ligand
vMIP-II
CX3CL1
[5P7]-CCL5
CCL20
CXCL8
[6P4]-CCL5
CCL5*
CCL3*
PDB
4RWS
4XT1
4XT3
5WB2
5UIW
6WWZ
6LFO
6LFM
7O7F
7F1R
7F1Q
Year
2015
2017
2020
2021

Figure 1

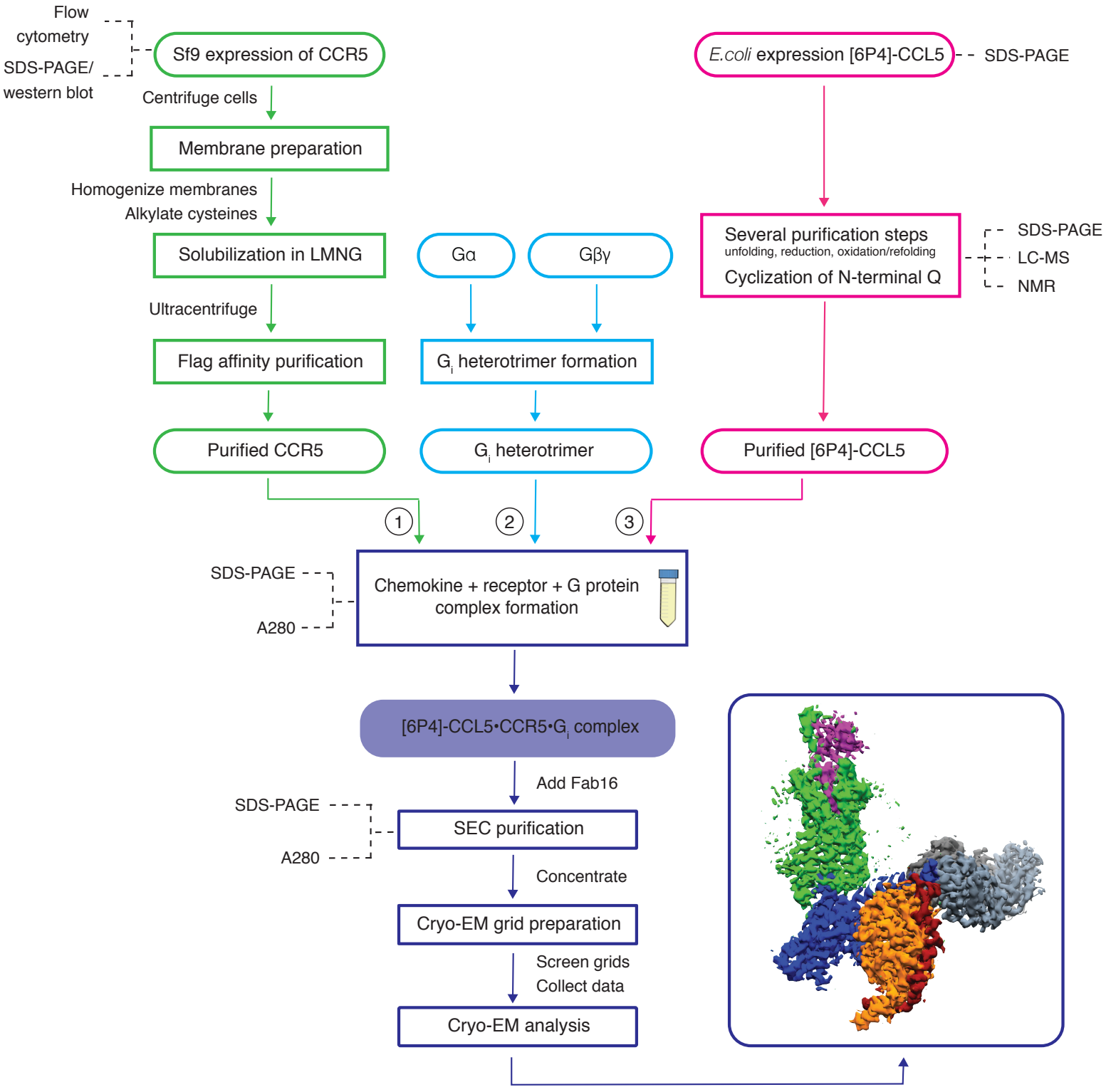
Flow cytometry
SDS-PAGE/ western blot
Sf9 expression of CCR5
Centrifuge cells
Membrane preparation
Homogenize membranes
Alkylate cysteines
Solubilization in LMNG
Ultracentrifuge
Flag affinity purification
Purified CCR5
Gα
Gβγ
G_i heterotrimer formation
G_i heterotrimer
E.coli expression [6P4]-CCL5
SDS-PAGE
Several purification steps
unfolding, reduction, oxidation/refolding
Cyclization of N-terminal Q
SDS-PAGE
LC-MS
NMR
Purified [6P4]-CCL5
1
2
3
SDS-PAGE
A280
Chemokine + receptor + G protein complex formation
[6P4]-CCL5•CCR5•G_i complex
Add Fab16
SDS-PAGE
A280
SEC purification
Concentrate
Cryo-EM grid preparation
Screen grids
Collect data
Cryo-EM analysis

Figure 2

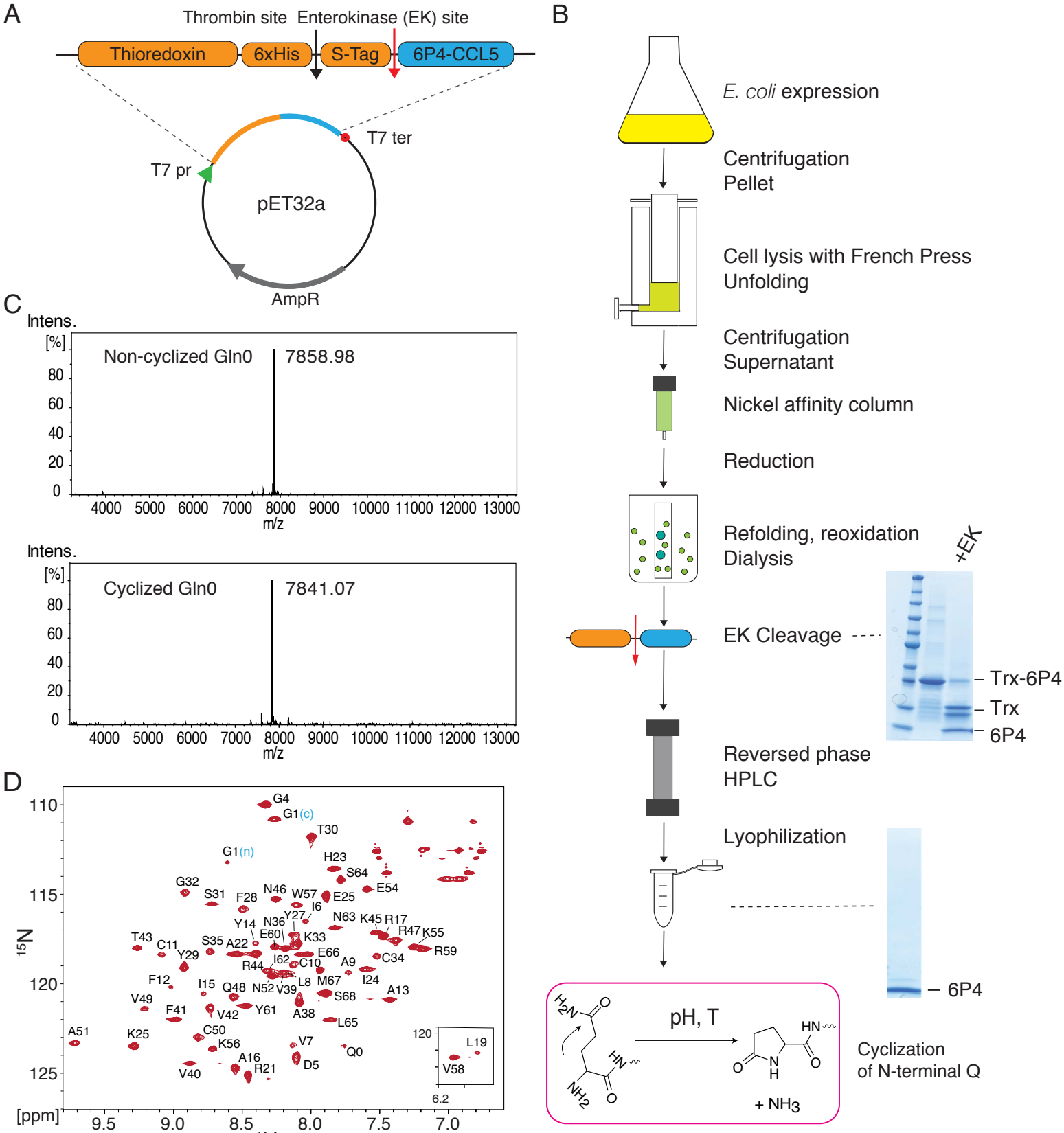
A
Thrombin site
Enterokinase (EK) site
Thioredoxin
6xHis
S-Tag
6P4-CCL5
T7 ter
T7 pr
pET32a
AmpR
B
E. coli expression
Centrifugation
Pellet
Cell lysis with French Press
Unfolding
Centrifugation
Supernatant
Nickel affinity column
Reduction
Refolding, reoxidation
Dialysis
EK Cleavage
+EK
Trx-6P4
Trx
6P4
Reversed phase
HPLC
Lyophilization
6P4
pH, T
+ NH3
Cyclization
of N-terminal Q
C
Intens.
[%]
Non-cyclized Gln0
7858.98
m/z
Cyclized Gln0
7841.07
D
15N
1H
[ppm]

Figure 3

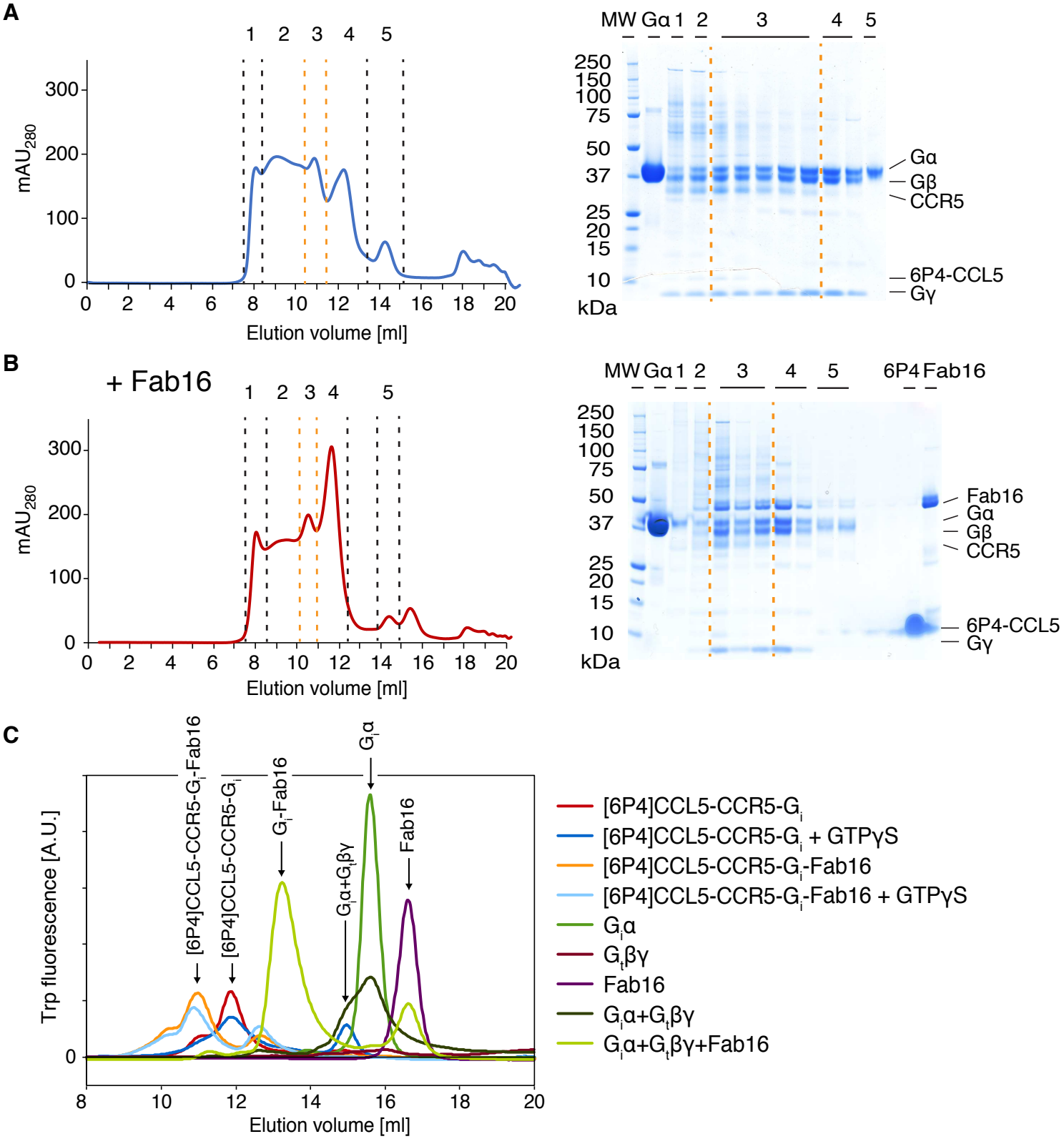
A
1 2 3 4 5
mAU280
300
200
100
0
0 2 4 6 8 10 12 14 16 18 20
Elution volume [ml]
MW Gα 1 2 3 4 5
250
150
100
75
50
37
25
20
15
10
kDa
Gα
Gβ
CCR5
6P4-CCL5
Gγ
B
+ Fab16
1 2 3 4 5
mAU280
300
200
100
0
0 2 4 6 8 10 12 14 16 18 20
Elution volume [ml]
MW Gα 1 2 3 4 5 6P4 Fab16
250
150
100
75
50
37
25
20
15
10
kDa
Fab16
Gα
Gβ
CCR5
6P4-CCL5
Gγ
C
[6P4]CCL5-CCR5-Gi-Fab16
[6P4]CCL5-CCR5-Gi
Gi-Fab16
Giα
Giα+Gtβγ
Fab16
Trp fluorescence [A.U.]
0
8 10 12 14 16 18 20
Elution volume [ml]
[6P4]CCL5-CCR5-Gi
[6P4]CCL5-CCR5-Gi + GTPγS
[6P4]CCL5-CCR5-Gi-Fab16
[6P4]CCL5-CCR5-Gi-Fab16 + GTPγS
Giα
Gtβγ
Fab16
Giα+Gtβγ
Giα+Gtβγ+Fab16

Figure 4